Delineation of the prostate capsule in 3D-Trans Rectal Ultrasound images using image registration.

S Mehta[a], DC Barber[b], E van Beek[c], JM Wild[c], FC Hamdy[c]

Royal Hallamshire Hospital, University of Sheffield, Glossop Road, Sheffield, S10 2JF.
[a]. Academic Urology, [b] Medical Physics, [c] Academic Radiology

Abstract: Detection of the penetration of the prostate capsule by prostate cancer is an important step in staging and managing this disease. Although the capsule cannot be directly visualised on 3D ultrasound images it is usually adjacent to a fat layer which becomes echolucent when penetrated by disease. Automatic detection of such regions requires firstly that the prostate boundary is automatically delineated. In this work this is done by defining a reference image and marking out the prostate boundary manually on this image. Patient images are then mapped to the reference and the inverse mapping used to map the reference boundary on to the patient image. The accuracy of this approach is evaluated by comparing subsections of the automatically generated boundary with equivalent manually defined boundary subsets generated on a small set of patient data. The median success factors, a measure of the overlap between automatic and manually defined boundaries, over 6 patients was 0.96 and the average linear displacement between the boundaries of the automatic and manual regions was 1.05 in units of pixel dimensions.

1 Introduction

Prostate cancer is a major public health issue. It is the second leading cause of male cancer death both in the USA and in Europe. Radical prostatectomy is a recognised and well-established treatment option for localised disease. Accurate staging is critical to the management of patients with prostate cancer. While prostatectomy is an appropriate procedure for patients in whom the disease is contained completely within the prostate capsule, it is ineffective for patients where disease has penetrated the capsule. Identification of penetration is therefore critical for effective management of the patient.. Current methods used for local staging include digital rectal examination, serum prostate specific antigen (PSA), Trans-Rectal Ultrasound (TRUS) with image guided biopsy, and endorectal magnetic resonance imaging (MRI). Trans-rectal ultrasound imaging is currently a standard procedure within the urology clinic. As part of this investigation biopsy samples are taken at various sites within the prostate, either guided by the visual observation of disease in the images, or systematically at selected sites within the prostate. Unless there is obvious disease external to the capsule prostate patients with disease confirmed by biopsy are referred for surgery and the prostate is removed. Conventional TRUS uses 2-D imaging to visualise a 3-D anatomy and disease process and has had limited success in staging prostate cancer. The introduction of 3-D TRUS offers a potentially improved way of visualising the prostate. 3D ultrasound imaging is a new imaging modality with potential still being explored. Volume images can be produced which are appropriate for post-imaging interpretation and manipulation through the use of appropriate image processing and analysis techniques. 3D data collection is currently in the form of a sequence of 2D image planes. The positions of these planes in space relative to each other needs to be determined. Methods of doing this include mechanical scanning and magnetic and optical position sensors. Mechanical scanning currently represents the most reliable form of data collection and using such a system good volume data sets can be obtained reliably and quickly within the Urology clinic.

A recent study by Garg *et al* [1] showed the benefits of 3-D imaging. Thirty-six patients with newly diagnosed clinically localised prostate cancer were studied. All patients underwent conventional trans-rectal ultrasonography (TRUS) with 3-D reconstruction. Images were interpreted blindly, and the findings were compared with histopathological staging following radical prostatectomy. Pathological staging of the specimens revealed 15 sites of extra-capsular extension in 10 patients, 8 of whom had positive margins. 3-D imaging identified 12 sites of extra-capsular extension in 9 patients with a positive predictive value of 90%.

A key requirement in staging prostate cancer is to identify if disease has penetrated the prostate capsule. The capsule itself cannot be visualised but is usually bordered by a layer of fat which shows up on the US image. If disease penetrates this fat layer it becomes locally echolucent. Accurate identification of such echolucent regions along the prostate boundary could help to stage disease more accurately and prevent ineffective surgery.

The proposed method of detecting echolucent regions is to identify the boundary of the prostate on the 3-D TRUS image and then render local values of image intensity onto this surface. Statistical or other methods can

be used to identify regions of abnormal intensity. To do this numerically the boundary of the prostate needs to be delineated. Manual identification and delineation of the prostate boundary is not feasible for routine clinical work. This paper describes a method being developed to locate the 3D prostate boundary automatically using image registration. Houston *et al* [2] proposed the use of 3D registration to delineate the boundary of 3D radionuclide cardiac studies. In their work the mapping function was an affine function, based on a previously published approach by Barber *et al* [3] for 3D image registration of brain radionuclide data. In both these cases the affine transform was adequate. However, registration of 3D-TRUS images of the prostate requires a non-linear mapping. Non-linear methods have been proposed using global basis functions (Friston *et al* [4], Barber [5]) but there are significant computational and other advantages in using local basis functions (Vemuri *et al*, [6]). Image registration has not been widely applied to ultrasound images because of the limited availability of 3D image data but Shields [7] investigated its use in removing motion effects when imaging the carotid artery though the cardiac cycle.

2 Methods

Six patients with proven prostate cancer without evidence of extra-capsular involvement were imaged using a Brüel and Kjæ 2102 ultrasound scanner with 3D imaging capability. Image data was transferred to a workstation for analysis. The data consisted of an angular sequence of 2D images, typically of dimensions 55 x 30 mm (pixel dimensions 0.13 x 0.13 mm) over an angle which could be selected by the user but was typically 125^{o}. The angular spacing between images was 0.3^{o}. Scanning took 20 seconds per data set. Data was stored for analysis in raw form without conversion from angular to Cartesian co-ordinates, but could be converted to Cartesian form for display purposes. Data was analysed in raw form. For the purpose of image registration data at high resolution is not required and so the image data in raw form is packed by summing 4 x 4 x 4 voxels to form a single voxel. The voxel dimensions are then 0.52 x 0.52 mm by 1.2^{o}. Once the mappings have been determined they can be applied to images of the original resolution, although this was not done here.

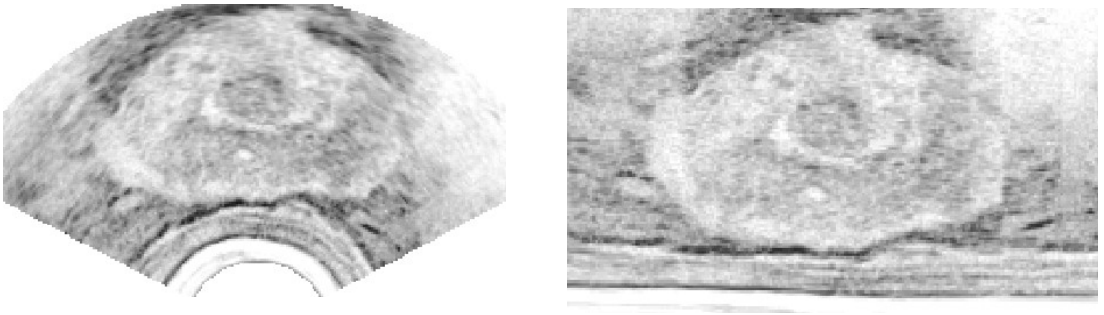

Figure 1. (a) Data in Cartesian form. (b) Data in raw form

Figure 1a shows a cross section through a 3-D scan of a prostate. Figure 1b shows the image data in raw form. The image is noisy and in many images the prostate border is poorly defined. The method used to identify the prostate boundary is to first construct a reference image, define a 3-D boundary on this image and then use image registration to map the boundary image to the patient image. A 3-D image registration algorithm (see Appendix for brief details) is first used to construct the reference image. A suitable patient image is chosen as a reference and the images from the remaining subjects registered to this reference image. The mean of the registered images is then computed and this is used as the reference image. A third cycle can be run if required

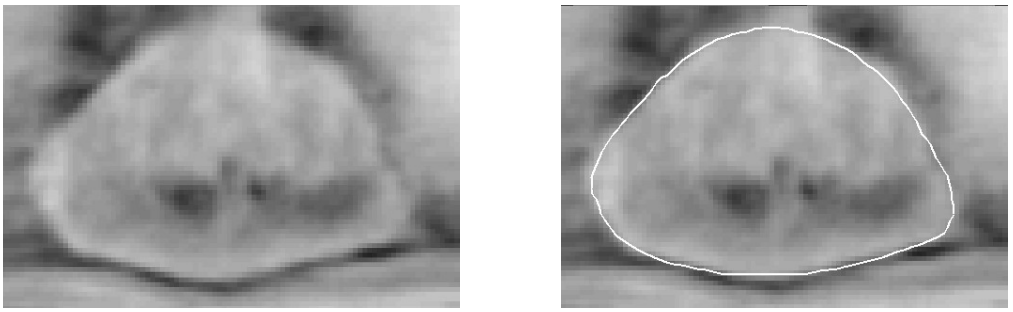

Figure 2 (a) The reference image (b) The reference boundary

but this usually produces few further changes. Figure 2a shows the reference image generated in this way from 6

subjects. A 3D reference boundary is then drawn on the reference image by hand. This can be a time consuming and potentially subjective process but only needs to be done once. Figure 2b shows a section of this boundary superimposed on the image of Figure 2a.

To define the boundary on a patient image the patient image is mapped to the reference image and the inverse mapping then used to map the reference boundary (defined as a binary image) back to the patient image. The boundary is mapped in this way for two reasons. The first is that in the algorithm used here (see appendix) the registration is driven by intensity gradients derived from the relatively low noise reference image rather than the noisy patient image. The second reason is that if the boundary is defined as a surface mesh then this mapping is in fact the correct mapping to map this mesh back to the patient image. In the present work the boundary image is a binary volume image and the inverse mapping needs to be calculated and used. Figure 3 shows a patient image with the mapped reference boundary (solid line) superimposed on the image.

The 'gold standard' is a manually generated boundary. Drawing full boundaries on a patient image is a time consuming process. For this preliminary study we have confined ourselves to manually delineating a subset of 6 sections through each set of patient data. These were drawn for all 6 subjects without reference to the automatic boundary. Figure 3 shows the manual boundary (dotted line) superimposed on the patient image along with the automatic boundary.

Two indices are used to define the accuracy of the segmentation. The first is the success factor (SF) proposed by Houston *et al* [2]. This is the area of the intersections of the corresponding regions divided by the average area of the two regions. The second, and for this project more appropriate, index is the average linear displacement (ALD) defined as the area of the differences between the two regions (the area of the exclusive or of the two regions) divided by the average of the perimeter lengths of the two regions. This is a value, in units of pixel dimensions, which can be interpreted as the average distance between the two boundaries. As manual boundaries have only been defined for a limited set of images in each data set these indices are calculated for each of these slices and the values averaged. A fully 3D version of the ALD would be to divide the volume of the difference by the average of the surfaces of the boundaries.

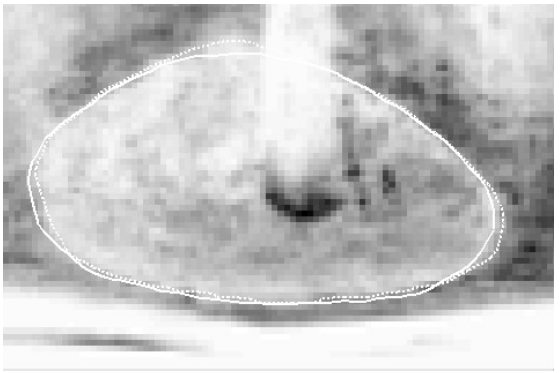

Figure 3 A subject image with manual (dotted) and automatic (solid) boundary superimposed

3 Results

The average SF taken over the six subjects was 0.96. The average ALD was 1.05. Computation time to map the full 3D boundary was just over a minute on a 2GHz PC.

4 Discussion

The aim of this preliminary project was to see if image registration could be used to delineate the 3D boundary of the prostate in a 3D TRUS image. Only a limited set of patient data has been analysed to date, but preliminary results suggest that delineation to the accuracy required should be achievable. In the present work only a limited amount of data was available and so the results must be interpreted with caution. In particular the reference image will reflect the characteristics of the small data set used. As more data is used to define the reference image this image will become more robust. It should also be possible to delineate the reference boundary more reliably. In this work the reference boundary has been defined manually on the reference image. Even on this image visual delineation of the boundary is not always clear. A better approach, though more labour intensive, is to delineate boundaries on a set of patient images, map these images, and hence the manual boundaries, to the reference image, and then take an average of these mapped boundaries. In this way, uncertainties in boundary delineation on individual subject may average out over a sufficiently large set of data. As with all image registration methods the image data need to be reasonably aligned to ensure correct convergence of the registration. It is simple to do this manually and in most images examine so far this does not have to be done too accurately, but fully automating initial alignment is a subject for further research.

5 Conclusion

Automatic delineation of the prostate boundary on 3D TRUS images seems feasible and could become a useful tool in the staging of prostate cancer. The method proposed is fully generic in that the domain specific knowledge required, the reference image and reference boundary, is independent of the computational algorithm used, and therefore the method should be applicable to other situations where 3D object boundaries are required.

References

1. S Garg, B Fortling, F C Hamdy. 1999 Staging of prostate cancer using 3-dimensional transrectal ultrasound images: a pilot study. *J Urol* , 162:1318-1321.
2. A S Houston, D White, W F D Sampson, M Mcleod and J Pilkington. 1998 An assessment of two methods for generation automatic regions of interest. *Nucl. Med. Commun* 19:1005-1016.
3. D C Barber, W B Tindale, E Hunt, A Mayes and H J Sagar. 1995 Automatic registrationof SPECT images as an alternative
4. to immobilisation in neuroactivation studies. *Phys Med Biol*. 40:449-463.
5. K J Friston, J Ashburn, C D Frith, J-B Poline, J D Heather and R S J Frackowiak 1995 Spatial registration and normalisation of images. *Human Brain Mapping* 2 165-189.
6. D C Barber 1999 Efficient nonlinear registration of 3D images using high order co-ordinate transfer functions *Journal of Medical Engineering & Technology*. 23:5 157-168
7. Vemuri B C, Huang S, Sahni S, Leonard C M, Mohr C, Gilmore R and Fitzimmons J 1998 An efficient motion estimator with application to medical image registration. *Medical Image Analysis* 2 79-98
8. K Shields, D C Barber and S B Sherriff. 1993 Image registration for the investigation of atherosclerotic plaque movement. In: Lecture notes in Computer Science 687. Information processing in Medical Imaging. H.H Barrett, A.F Gmitro (eds.) Springer-Verlag 438-458

Appendix

The aim of registration is to map an image m(x,y,z), the moved image, to an image f(x,y,z), the fixed image. We assume that such a mapping is possible in that there is a one-to-one mapping which converts m(x,y,z to f(x,y,z) such that the intensity values completely match (in the absence of noise). Then the moved and fixed images can be related by

$$m(x+\Delta x(x,y,z), y+\Delta y(x,y,z), z+\Delta z(x,y,z)) = f(x,y,z)$$

where $\Delta x(x,y,z)$, $\Delta y(x,y,z)$ and $\Delta z(x,y,z)$ together constitute the mapping function.

We modify the above equation by adding an extra term

$$m(x+\Delta x(x,y,z), y+\Delta y(x,y,z), z+\Delta z(x,y,z)) - \Delta s(x,y,z) = f(x,y,z)$$

which deals with the residual differences between the two images. In this form, the mapping function (including the $\Delta s(x,y,z)$ term) is clearly non-unique. However, if smoothness constraints are imposed on the mapping functions unique solutions are possible. One such constraint is to expand the mapping functions in terms of a set of basis functions $\phi_i(x,y)$. We can show that, for images close together

$$f(x,y,z)-m(x,y,z) = \frac{1}{2}\Delta x(x,y,z)\left[\frac{\partial f}{\partial x}+\frac{\partial m}{\partial x}\right]+\frac{1}{2}\Delta y(x,y,z)\left[\frac{\partial f}{\partial y}+\frac{\partial m}{\partial y}\right]+\frac{1}{2}\Delta z(x,y,z)\left[\frac{\partial f}{\partial z}+\frac{\partial m}{\partial z}\right]-\Delta s(x,y,z) \qquad (1)$$

and by expanding the components of the mapping function in terms of basis functions $\phi_i(x,y,z)$

$$f(x,y,z)-m(x,y,z) = \frac{1}{2}\sum_{\text{all i}} a_{xi}\phi_i(x,y,z)\left[\frac{\partial f}{\partial x}+\frac{\partial m}{\partial x}\right]+\frac{1}{2}\sum_{\text{all i}} a_{yi}\phi_i(x,y,z)\left[\frac{\partial f}{\partial y}+\frac{\partial m}{\partial y}\right]+\frac{1}{2}\sum_{\text{all i}} a_{zi}\phi_i(x,y,z)\left[\frac{\partial f}{\partial z}+\frac{\partial m}{\partial z}\right]-\sum_{\text{all i}} a_{si}\phi_i(x,y,z)$$

which can be solved for the parameters **a**. Additional smoothing constraints in terms of minimising the magnitude of the Laplacian of the mapping function can also be added. The basis functions used in this work are local bilinear functions.

Inclusion of the $\Delta s(x,y,z)$ without constraint results in a trivial solution in that $\Delta s(x,y,z)$ can be set to f – m. However, consider equation 1. The difference between f and m is made up of contributions from four terms. If each of these terms contributes equal amounts to the differences between f and m then since the gradients are relatively non-smooth functions Δx and Δy will be smoother than Δs. The *smoothest* way of accounting for the difference between f and m is as far as possible to utilise the first two terms and then evoke Δs when all else fails. This is what appears to happen in practice. The Laplacian smoothness constraint is not shown in the above analysis but is added in the context of solving the **a** in the usual way. The mapping functions are computed using image data within a registration region around the prostate.